Journal of Materials Chemistry A

Accepted Manuscript

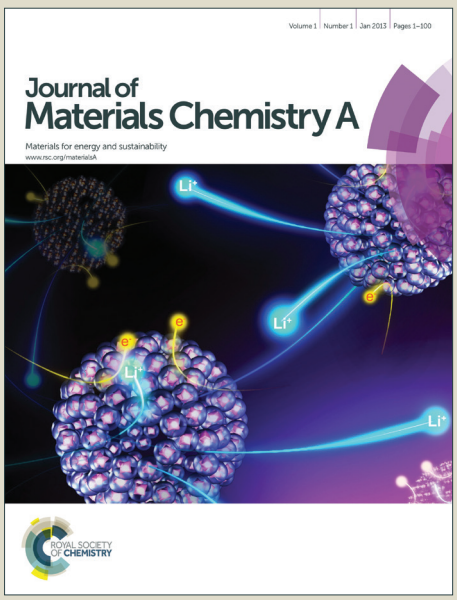

ROYAL SOCIETY OF CHEMISTRY

www.rsc.org/materialsA

Highly efficient nitrate ester explosives vapor probe based on multiple triphenylaminopyrenyl-substituted POSS

Yixun Gao[a,b], Wei Xu[a,c], Defeng Zhu[a], Lei Chen[a,b], Yanyan Fu[a], Qingguo He[a*], Huimin Cao[a] and Jiangong Cheng[a*]

[a]State Key Lab of Transducer Technology, Shanghai Institute of Microsystem and Information Technology, Chinese Academy of Sciences, Changning Road 865, Shanghai 200050, China. E-mail: hqg@mail.sim.ac.cn; jgcheng@mail.sim.ac.cn.

[b]University of the Chinese Academy of Sciences, Yuquan Road 19, Beijing,100039, China

[c]Shanghaitech University, No.8 Building, 319 Yueyang Road, Shanghai 200031, China

Abstract

Compared with nitroaromatic explosives detection, nitrate ester explosives are far from broad attention possibly due to their absence of aromatic ring and difficulty in being detected. An eight triphenylamino-pyrenyl substituted POSS **(P8PT**) was designed as the sensory material. POSS was chosen as the skeleton due to its nano structure, multiple reactive sites, structure similarity with nitrate esters and high thermal stability, which will contribute to large surface area induced high sensitivity, tunable sensory units number, stronger interaction force with nitrate esters and high stability. For comparison, triphenylamino-pyrene (**Py-TPA**) (without POSS), one and three Py-TPA substituted POSS were also synthesized and characterized. Their chemical structures, photophysical and electrochemical properties show that the **P8PT** has a 3-D symmetrically spacial conformation, higher molar extinction coefficient, higher area-to-volume ratio, multiple exciton transfer path, and matched energy level with nitrate ester explosives, which will all contribute to highly efficient sensing performance and nice selectivity for nitrate ester explosives such as nitroglycerin (NG) detection. The fluorescence of the P8PT film is 63% quenched upon exposure to a saturated vapor of NG for 50 s and 92% quenched for 300 s at room temperature due to photoinduced electron transfer between the probe and NG. These results reveal that P8PT is suitable for preparing a highly sensitive and efficient thin-film device for detecting nitrate esters.

KEYWORDS: Fluorescent probe, POSS, Nitrate esters, Photoinduced electron transfer

1. Introduction

In recent years, the development of recognition and sensing systems for the detection of explosives has received considerable attention in the fields of national security and military use.[1-3] Currently, detection technologies of trace explosives include GC-MS,[4] nuclear quadrupole resonance (NQR),[5] surface-enhanced Raman spectroscopy,[6] cyclic voltammetry,[7] etc. With their own advantages and adaptability to analyze suspicious materials, these methods still have some shortcomings and negative factors, such as cumbersome analysis process, expensive and complicated equipments, serious interference and robust portability.

Nitroglycerin (NG) is a classic nitrate ester which has been used as an active ingredient in the manufacture of explosives and military firearms. Compared with nitroaromatic explosives detection, nitrate ester exlosives are far from wide attention possibly due to their shortage of aromatic ring and difficulty to be detected. J. Thomas et al reported the application of ultra performance liquid chromatography tandem mass spectrometry (UPLC/MS/MS) method which can detect NG and 17 other explosives in a total of 20 different components under 8 min.[8] W. Fan and J. Almirall reported the improvement of the headspace analysis of NG, 2,4-DNT, and diphenylamine by using capillary microextraction of volatiles (CMV).[9] A. Zalewska and co reported a 100 ng detection limit of NG by using two types of handheld trace explosives detectors, which are based on ion mobility spectrometry (IMS) and field asymmetric ion mobility spectrometry (FAIMS), relatively.[10] H. Guan et al reported a rapid detection method of NG and other nitro explosives in water using disposable

pipette extraction followed by HPLC.[11] However, these methods of detection also have their own deficiencies as mentioned above. Therefore the development of novel sensory materials with superior performance and detection methods for trace nitrate esters detection are at the heart of current interest.

Fluorescent conjugated polymers generally exhibit high sensibility than that of small molecules due to molecular wire effect[12] and their facile thin film device fabrication via a simple spin coating. However, the problems of polymers lie in that they generally suffer from a broad molecular weight dispersion and catalyst residue resulting in batch to batch difference and poor stability,[13] while small molecules could be easily purified via column separation or vacuum sublimation. Our interests are to find some small molecule sensory materials with high sensitivity, high stability and facile film fabrication.

Recently, polyhedral oligomeric silsesquioxanes (POSS) with rigid cage-like nanostructures consisting of an inorganic Si-O-Si core were commonly used for luminescent material design to increase the thermal stability and decrease the aggregation triggered fluorescence quenching.[14-18] We plan to introduce POSS as the skeleton of the sensory material for three reasons. One is the natural nano structure could endow the sensory material with high surface area, which could improve the sensitivity. The second is various numbers of luminescent units could be introduced to systematically investigate the relationship between the number of luminescent units and the sensing performance due to its eight reactive sites.[19] The third is to increase the interaction force strength with the nitro esters and hence to increase the sensitivity.

Our consideration is nitrate esters are non aromatic and polar, the non polar aromatic luminescent units lack of structural similarity with them, and the interaction force will be poor, while the polar POSS skeleton will greatly increase the interaction force between them. In addition, POSS also could be used to increase the thermal stability, which is important for long lifetime of the sensory device.

For the luminescent sensory unit selection, because compared with electron deficient aromatic explosive such as TNT, nitrate esters have higher LUMO level, the sensory units should have much higher LUMO level than nitro-aromatic explosive sensing materials.[20] Pyrene and its derivatives are widely used in recent research on chemical sensors, which have high molar extinction coefficient and fluorescence quantum yield, and more importantly, the high LUMO level. But molecules with multi-pyrene units are often suffered from the aggregation triggered fluorescence quenching effects and poor photostability. A triphenylamine (TPA) group could well solve such problems for its propeller spatial structure and electron donating character.[21] Therefore, to improve the fluorescence efficiency, we introduced TPA units.

With this in mind, we intended to synthesis a multiple TPA-Pyrenyl substituted POSS structure as a sensory material (**Fig. 1**) towards NG via Pd-catalyzed Suzuki coupling and Heck coupling reactions. For comparison, the luminescent sensory material with no POSS units (**Py-TPA**), the materials with one (**P1PT**), three (**P3PT**) and eight luminescent units (**P8PT**) were synthesized for a systematical investigation of the relationship between the molecular structure and the sensing performance.

2. Experimental section

All chemicals and solvents were obtained from commercial sources and used as received without further purification. Polyhedral octavinylsilsesquioxane (purity, 95%) was bought from Aladdin Industrial Corporation. UV-Vis absorption and fluorescence analysis were obtained from a Jasco V-670 spectrophotometer and a Jasco FP 6500 spectrometer, respectively. Decomposition points were recorded on a differential scanning calorimeter (DSC, TA Instruments Q10) at a scan rate of 5 ºC/min. Elemental analyses (C, H, N) were performed on a Vario EL III Elemental Analyzer. Cyclic voltammetry (CV) experiments were performed with a CH Instruments electrochemical analyzer. The electrochemical behaviors of products as well as the nitrate esters were investigated in a standard three electrode electrochemical cell with 0.1 M tetra-*n*-butylammonium hexafluorophosphate (Bu_4NPF_6) in acetonitrile solution, (a glassy carbon working electrode, a platinum counter electrode and a saturated calomel electrode as a reference electrode) and the scanning rate was 100 mV/s under nitrogen atmosphere at room temperature.

Synthesis of POSS-xPyTPA

TPA-Py-Br was synthesized by 1,6-dibromopyrene and 4-(N,N-diphenyl)aminophenylboronic acid pinacol ester through Suzuki cross-coupling reaction, using tetrakis(triphenylphosphine) palladium ($Pd(PPh_3)_4$) as catalyst.

Polyhedral octavinylsilsesquioxane (POSS) (0.3 mmol, 190 mg),

4-(6-bromopyrenyl)-triphenylamine (TPA-Py-Br) (2.5 mmol, 1.3 g), and $Pd_2(dba)_3$ (0.093 mmol, 85 mg) were placed in an oven-dried round bottom Schlenk flask. A mixture of freshly dried dioxane (40 mL), N,N-dicyclohexylmethylamine (22.5 mmol, 4.85 mL) and Tri-*tert*-butylphosphine (1 M solution, 0.2 mmol, 0.2 mL) was added to the degassed flask. The reddish brown mixture was stirred at 85 ºC for 48 h. After cooling to room temperature, it was then filtered and the filtrate was poured into methanol. The precipitate was collected and purified by column chromatography using dichloromethane and petroleum ether as eluent with a ratio of 1:4. After drying, 588 mg yellow powdered **POSS-8PyTPA (P8PT)** was obtained in a yield of 47%. ^{1}H NMR (500M, $CDCl_3$, ppm): δ 6.98 (s, 4H), 5.01 (s, 2H), 9.21-7.62 (m, 25H), 7.62-6.49 (m, 67H), 6.49-5.82 (m, 3H). Elemental analysis (%) calcd for $C_{288}H_{192}O_{12}N_8Si_8$: C, 82.76; H, 4.59; N, 2.68; found: C, 79.26; H, 5.06; N, 2.68. MALDI-MS calcd. for $C_{288}H_{192}O_{12}N_8Si_8$: 4176.6; found: 4175, 3732, 3289.

Similar method was used for the synthesis of **POSS-PyTPA** and **POSS-3PyTPA**, with yields of 62% and 48%, relatively. **POSS-PyTPA (P1PT)**: ^{1}H NMR (500 M, $CDCl_3$, ppm): δ 8.40 (d, 1H, J=5 Hz), 8.35 (t, 1H, J=9.5 Hz), 8.26 (d, 1H, J=4.5 Hz), 8.23 (d, 1H, J=3.5 Hz), 8.16 (d, 1H, J=3.5 Hz), 8.07 (q, 2H, J=7 Hz), 8.02 (t, 2H, J=7 Hz), 7.51 (t, 2H, J=8.5 Hz), 7.33 (t, 4H, J=7 Hz), 7.28-7.22 (m, 6H), 7.08 (t, 2H, J=7 Hz), 6.47 (q, 1H, J=8 Hz), 6.20-5.93 (m, 25H). MALDI-MS calcd. for $C_{288}H_{192}O_{12}N_8Si_8$: 1076; found: 1074.9. **POSS-3PyTPA (P3PT)**: ^{1}H NMR (500M, $CDCl_3$, ppm): δ 6.98 (s, 4H), 5.01 (s, 2H), 9.21-7.62 (m, 25H), 7.62-6.49 (m, 67H), 6.49-5.82 (m, 3H). MALDI-MS calcd. for $C_{288}H_{192}O_{12}N_8Si_8$: 1961; found: 1963.9,

1519.8

Synthesis of Py-TPA

Py-TPA was synthesized through similar Suzuki cross-coupling reaction. Boronic acid pinacol ester pyrene (1 mmol, 230 mg), 4-bromo-triphenylanime (1.2 mmol, 346 mg) and $Pd(PPh_3)_4$ (0.1 mmol, 101 mg) were placed in an oven-dried round bottom Schlenk flask. A mixture of dried tetrahydrofuran (20 mL) and potassium carbonate solution (5 mL, 2 mol/L) was added to the degassed flask. The light-yellow mixture was stirred at 75 ºC for 24 h. After cooling to room temperature, the mixture was extracted with dichloromethane, washed with water, and dried by magnesium sulfate. The filtrate was collected and purified by column chromatography using dichloromethane and petroleum ether as eluent with a ratio of 1:4. After drying, **Py-TPA** (320 mg, 72% yield) was obtained as light yellow powder. ^{1}H NMR (500M, $CDCl_3$, ppm): δ 8.29 (d, 1H, J=9.4 Hz), 8.19 (t, 1H, J=5 Hz), 8.16 (d, 2H, J=9.3 Hz), 8.08 (s, 2H), 8.04 (d, 1H, J=13.8 Hz), 8.00 (t, 2H, J=6 Hz), 7.56 (d, 2H, J=8.5 Hz), 7.32 (t, 4H, J=7.5 Hz), 7.24 (t, 6H, J=9 Hz), 7.07 (t, 2H, J=7.5 Hz); ^{13}C NMR (500M, $CDCl_3$, ppm): 137.46, 134.99, 131.52, 131.37, 131.02, 130.38, 129.36, 128.45, 127.63, 127.44, 127.33, 127.28, 125.98, 125.42, 125.02, 124.73, 124.70, 124.61, 123.29, 123.05. Elemental analysis (%) calcd for $C_{34}H_{23}N$ (455.2): C, 91.65; H, 5.20; N, 3.14; found: C, 91.67; H, 5.20; N, 3.17. MALDI-MS calcd. for $C_{34}H_{23}N$: 455.2; found: 454.

Vapor sensing experiment

The fluorescence quenching experiments of the sensing films towards nitrate ester explosive vapors were conducted as follows: a small amount of explosives or interferents (3 mg for solid or 3 μL for liquid) was placed in a 1 cm quartz cell with absorbent cotton covered to prevent direct contact of explosives and maintain a constant saturation vapor pressure. The sensing films were prepared by dip-coating a tetrahydrofuran solution of each material onto a 10 × 20 mm quartz plate and vacuum-dried for half an hour before use. With the sensing film inserted, the cell was placed in the fluorescence spectrometer. The emission data were collected at certain times in a wavelength region of 470-520 nm with an excitation wavelength of 380-390 nm, while the slit width of excitation and emission are 1 mm and 5 mm relatively.

3. Result and discussion

Synthesis and characterization

All the materials here used were characterized by Nuclear Magnetic Resonance (NMR) and Mass spectra (MS). According to the matrix assisted laser desorption ionization-time-of-flight (MALDI-TOF) results, the as-synthesized sample P8PT contains eight, seven and six substituted substances. And P3PT is composed of both three and two substituted substances, While P1PT has only one-substituted target. All the as-synthesized samples were used directly for the sensing experiments.

Optical properties

P8PT is soluable in THF and CH_2Cl_2, but in other common solvents, such as

toluene and acetone, it demonstrates a poor solubility. The photophysical properties in solution were taken from its THF solution with a concentration of 10^{-6} M. And the spin-coated film was fabricated onto quartz plates from its THF solution with a concentration of 4×10^{-5} M. For comparison, all the optical data of the luminescent material without POSS and with one, three and eight luminescent units substituted POSS were summarized in **Table 1**, corresponding UV-Vis and fluorescence spectra in solution and film were shown in **Fig. 2**.

It can be seen from Table 1 and Fig.1, the absorption and emission peaks of the materials with POSS are all red shifted relative to those of **Py-TPA** in solution, around 24 nm for the absorption peak and 40 nm for the emission peak. It is easy to interpret since all the materials with POSS contain one more double bonds. Thus the conjugation length is expanded with it, and silicon atom directly linked with double bond may also contribute to the spectral red shift.

Fig. 2 also indicates that, among the materials with POSS structure, the normalized absorption and emission spectra almost completely overlapped with each other, demonstrating that there is almost no electronic or energy interaction between the two neighboring TPA-Py units inside the molecule. However, the number of the luminescent units does affect their molecular extinction coefficient (MEC). The MEC of **P8PT** is 7.94 fold that of **P1PT**, and 6 fold that of **P3PT**. It is also mentionable that for **P3PT** and **P1PT**, the MEC is lower than **Py-TPA** for its lower luminescent chromphore density due to the introduction of POSS.

Unlike the absorption spectral change in solution, the materials with POSS units

in film state showed a different extent of red shift relative to **Py-TPA**. For **P1PT** and **P3PT**, the red shifts of their absorption peaks are only 7 and 11 nm relatively, but for **P8PT**, the red shift quickly rises to 38 nm, and the whole absorption spectrum showed a 40 nm translation. Such a big red shift means there is stronger intermolecular interaction inside **P8PT** film than that of **P1PT** and **P3PT**. As compared, their emission spectra exhibit a similar change, all the materials with POSS unit emit at 515 nm with a 40 nm red shift relative to that without POSS unit. As for fluorescent sensing of conjugated polymer in film state, the interchain interaction could provide more efficient exciton transport and herein result in much efficient sensing efficiency.[12] Also for small molecules, moderate intermolecular interaction may also be critical for efficient exciton transport. In this point, we believe **P8PT** will be a nice candidate for such explosive sensing.

Electrochemical properties

For an explosive sensing material via photo induced electron transfer (PET) mechanism, one important factor is its LUMO level. The cyclic voltammetric curves of all the sensory materials were measured to get the HOMO and LUMO levels, and their energy gaps were calculated. The data were summarized in **Table 1**. It could be seen that LUMO level of **P8PT** (-2.77 ev) is higher than that of NG (-3.39 ev) and other nitrate ester explosives. These indicate the possibility of PET from the probes to the nitrate esters. In other words, **P8PT** can be used as the fluorescent probe for nitro esters including NG detection.

Thermostability

As designed, we suppose the introduction of POSS unit could efficiently increase the thermal stability of the probe, which is the basis for a sensing device with a long lifetime.[22, 23] Thermogravimetric analysis (TGA) showed that the decomposition temperature of **P8PT** is over 480 ºC, while that of **Py-TPA** will decompose at 390 ºC. A more than 90 ºC enhancement means POSS unit could efficiently improve the thermal stability of the probe, which can be a nice candidate for a long lifetime device in practical application.

Fluorescence quenching study and structural analyse

The emission spectra of all the probes under air and nitrate ester explosives vapor with time were monitored, as shown in **Fig. 3** and **Table 2**. As expected, sensory materials with POSS units demonstrate far better quenching efficiency compared with that without POSS. Only 6% of its emission peak intensity was decreased upon exposure to NG at 300 s for **Py-TPA**. While **P1PT** has a 66% quenching under the same condition, there is ten folds increase related to **Py-TPA**. A further change to **P3PT** corresponds to a further 7% increase. The most prominent quenching efficiency was observed for **P8PT**. The fluorescence of **P8PT** decreased with **63**% in 50 s, and 92% in 300 s.

Three points could be found in the results. Firstly, **Py-TPA** demonstrated very poor sensory response to NG. We think it comes from its poor structural similarity with NG. As pointed in the introduction part, NG has no aromatic rings and has three very polar nitro units, while **Py-TPA** is aromatic and the polarity is very weak compared with NG, which make them unfavorable to come near to each other.

Therefore, although the LUMO level of **Py-TPA** is higher than that of NG, the PET process can only occur between very few molecules. Secondly, POSS structure is critical in NG sensing as expected due to its nano structure, which results in high surface to volume ratio and much structural similarity between POSS and NG. That is why all three probes with POSS units demonstrated much better sensing performance. Thirdly, the sensing is highly related to the number of the luminescent units, the more the luminescent units, the better sensing performance. **P8PT** showed far better quenching efficiency than **P1PT** and **P3PT** at a time longer than 25 s. To interpret its special sensing behavior, we have to recall its absorption spectrum in film state. As described, it is red shifted about 40 nm relative to **P1PT** and **P3PT**, we propose it should be related to a special aggregation, which could make the exciton transfer more efficiently. And integrated with its molecular structure, such an aggregation should be related to intermolecular interchain interaction. For **P8PT**, the eight **Py-TPA** units will extend to eight different spatial directions, which will greatly increase the pathways for exciton transfer. [24]

To further prove our assumption that the intermolecular aggregation induced special sensing behavior, we performed the molecular dynamic calculation based on Material Studio software.[25] The details for calculation are provided in the supporting information. Eight **P8PT** molecules were put inside one lattice and proceeded with 10,000 steps. Results were shown in **Fig. 4**. As expected, eight **Py-TPA** units take eight directions for steric hindrance. Between two **P8PT**, due to the pyramidal structure of TPA, they could not well pack with each other by strong π-π interaction,

but rather take as C-H···π interaction. The nearest distance between the end of one phenyl ring and another phenyl ring is around 3.620 Å, which could provide insights for its special sensory behavior.

As the thin film sensing device, surface morphology of **POSS-xPyTPA** will be highly related to the sensing efficiency, which is investigated by SEM tests. As shown in **Fig.5**, **P8PT** demonstrate a quite different morphology, the film is mainly composed of very large particles with diameters of around 500 nm and the up surfaces are quite flat. In contrast, **P1PT** and **P3PT** films are obviously formed of random small particles. We suppose it comes from their different molecular structure, **P8PT** are highly symmetry, while **P1PT** and **P3PT** are asymmetry, unsymmetrical intermolecular force make it form random particle (see supporting information). These results give a direct proof of its special absorption spectrum in film state, which exhibits a very special aggregation.

Concentration effect in film fabrication

As the thin film probe, the thickness of the film will also highly influence its sensing performance. The concentration was tuned from 1×10^{-4} to 5×10^{-6} mol/L in THF to afford the thin film device with different thickness. The sensing efficiency at 300 s was shown in **Fig.6**. As can be seen, the film from a concentration of 4×10^{-5} mol/L gave the highest quenching efficiency (92%). SEM was also used to give insight into the morphology of films prepared from different concentrations, as shown in **Fig.7**. We found that the film from 4E-5 mol/L demonstrates a rather continuous and porous structure. Higher concentrations result in thicker films and worse vapor

penetrability, while the thinner concentrations induce randomly dispersed small nano particles lacking the continuity of films, which seriously influence their sensory performance.

Selectivity of sensing materials

To explore the potential applications of **P8PT** as a sensory material for nitrate esters detection, a series of nitrate esters and other commonly found interferents were adopt for the selectivity comparison as shown in **Fig. 8**. It could be found that **P8PT** showed nice response to nitrate esters, but almost mo response to common interferents, such as ethanol, tetrahydrofuran, acetone and toluene etc. Besides NG, **P8PT** also has a 68% fluorescence quenching in glycol dinitrate vapor, and more than 30% in methylnitrate and ethylnitrate. It can even response to **PETN**, which has a saturated vapor of only 1.82×10^{-6} Pa (5.67 ppt). Within the nitrate esters, the response is related with the electron-withdrawn capacity and vapor pressure of the nitrate esters. NG have three nitro units, which endow it nice electron-withdrawn capacity, although the vapor pressure 0.223 Pa (500 ppb) is far lower than that of methylnitrate and ethylnitrate, the sensory performance is far better than them. And for PETN, although vapor pressure is very low, a 10% quenching could be realized. The results show that the sensing films have good selectivity towards nitrate ester explosives and might be developed for nitrate ester explosive detection.

4. Conclusion

In summary, we developed a new fluorescent probe **P8PT** with POSS as skeleton

and eight triphenylamino-pyrene units as sensing chromophores for sensitive and selective detection of nitrate ester explosives vapor. Compared with the sensory material without POSS, **P8PT** has 5.2 times of molar extinction coefficient and 90 ºC increased thermal decomposition temperature. More importantly, even **P1PT** showed ten folds quenching efficiency of **Py-TPA** upon exposure to NG vapor due to photo induced electron transfer. The highest quenching efficiency was found for **P8PT**, which demonstrated an efficiency of 63% in 50 s, and 92% in 300 s upon exposure to saturated NG vapor at room temperature.

All the results support that the nano size and structure of POSS could enhance the interaction force of the sensory material and nitrate esters, as well as the surface to volume ratio of the sensory film, which contributes to the highly efficient sensory performance to nitrate esters. The sensing performance is highly related to the number of the luminescent units, the more the luminescent units, the better sensing performance. **P8PT** showed far better quenching efficiency due to its special intermolecular interaction resulted in multiple exaction transfer path, which could make the exciton transfer more efficiently.

In addition, parallel tests of other nitrate esters and common analytes proved **P8PT** has high selectivity and low disturbance from the common interferents. This rapid, simple and low-cost method provides a new route for trace and on-site detection of nitrate ester explosives, which has great relevance to human health, public safety and national defense.

5. Acknowledgements

We thank the research programs from the National Natural Science Foundation of China (No. 21273267, 61325001,61321492 and 51473182), Ministry of Science and Technology of China (Program No. 2012BAK07B03), and Shanghai Science and Technology Committee (Grant No. 11JC1414700).

6. References

1) J. Wang, *Analytica Chimica Acta*, 2004, 507, 3-10.
2) S.-I. Ohira and K. Toda, *Analytica Chimica Acta*, 2008, 619, 143-156.
3) I. A. Buryakov, T. I. Buryakov and V. T. Matsaev, *Journal of Analytical Chemistry*, 2014, 69, 616-631.
4) D. S. Moore, *Rev Sci Instrum*, 2004, 75, 2499-2512.
5) V. P. Anferov, G. V. Mozjoukhine and R. Fisher, *Rev Sci Instrum*, 2000, 71, 1656-1659.
6) J. M. Sylvia, J. A. Janni, J. D. Klein and K. M. Spencer, *Analytical chemistry*, 2000, 72, 5834-5840.
7) M. Krausa and K. Schorb, *J Electroanal Chem*, 1999, 461, 10-13.
8) J. L. Thomas, D. Lincoln and B. R. McCord, *Journal of forensic sciences*, 2013, 58, 609-615.
9) W. Fan and J. Almirall, *Analytical and bioanalytical chemistry*, 2014, 406, 2189-2195.
10) A. Zalewska, W. Pawlowski and W. Tomaszewski, *Forensic science international*, 2013, 226, 168-172.
11) H. X. Guan and K. Stewart, *Anal Lett*, 2014, 47, 1434-1447.
12) S. W. Thomas, G. D. Joly and T. M. Swager, *Chem Rev*, 2007, 107, 1339-1386.
13) D. A. Pardo, G. E. Jabbour and N. Peyghambarian, *Adv Mater*, 2000, 12, 1249-1252.

14) D. B. Cordes, P. D. Lickiss and F. Rataboul, *Chem Rev*, 2010, 110, 2081-2173.

15) X. H. Yang, J. D. Froehlich, H. S. Chae, B. T. Harding, S. Li, A. Mochizuki and G. E. Jabbour, *Chem Mater*, 2010, 22, 4776-4782.

16) W. Zhang and A. H. E. Mueller, *Progress in Polymer Science*, 2013, 38, 1121-1162.

17) K. Tanaka and Y. Chujo, *Polymer Journal*, 2013, 45, 247-254.

18) H. Hussain and S. M. Shah, *Polymer International*, 2014, 63, 835-847.

19) J. H. Jung, J. C. Furgal, T. Goodson, T. Mizumo, M. Schwartz, K. L. Chou, J. F. Vonet and R. M. Laine, *Chem Mater*, 2012, 24, 1883-1895.

20) L. Chen, Y. X. Gao, Y. R. Wang, C. He, D. F. Zhu, Q. G. He, H. M. Cao and J. G. Chengt, *Acs Appl Mater Inter*, 2014, 6, 8817-8823.

21) C. He, D. Zhu, Q. He, L. Shi, Y. Fu, D. Wen, H. Cao and J. Cheng, *Chemical communications*, 2012, 48, 5739-5741.

22) J. D. Froehlich, R. Young, T. Nakamura, Y. Ohmori, S. Li, A. Mochizuki, M. Lauters and G. E. Jabbour, *Chem Mater*, 2007, 19, 4991-4997.

23) M. Y. Lo, C. G. Zhen, M. Lauters, G. E. Jabbour and A. Sellinger, *Journal of the American Chemical Society*, 2007, 129, 5808-+.

24) Y. Wang, A. La, Y. Ding, Y. X. Liu and Y. Lei, *Adv Funct Mater*, 2012, 22, 3547-3555.

25) A. C. Khazraji and S. Robert, *Journal of Nanomaterials*, 2013, DOI: 10.1155/2013/409676.

Figure captions

Fig. 1 Chemical structures of **Py-TPA** and **POSS-xPyTPA**.

Table 1 Optical properties and energy level data of **P8PT** and **Py-TPA**.

Fig.2 UV-Vis absorption and fluorescence spectra of Py-TPA and POSS-xPyTPA in THF (1×10^{-5} M) (a) and spin-coating films on quartz (b).

Table 2 Optical properties and quenching efficiencies toward NG of **POSS-xPyTPA** and **Py-TPA**.

Fig.3 Sensing properties of **Py-TPA, P1PT, P3PT** and **P8PT** film toward saturated NG vapor.

Fig.4 Calculation results of eight **P8PT** molecules in a lattice after 10,000 steps. (use Forcite in Material Studio)

Fig.5 SEM images of **P1PT** (a), **P3PT** (b) and **P8PT** (c) films. All the films were spin coated from their THF solutions with a concentration of 4×10^{-5} mol/L.

Fig.6 Quenching efficiency of **P8PT** in 300 s from its THF solution of different concentrations for spin-coating.

Fig.7 SEM images of **P8PT** films spin coated from its THF solutions of different concentrations (marked on the images).

Fig.8 Selectivity of **P8PT** towards a series of nitrate esters and common interferents.

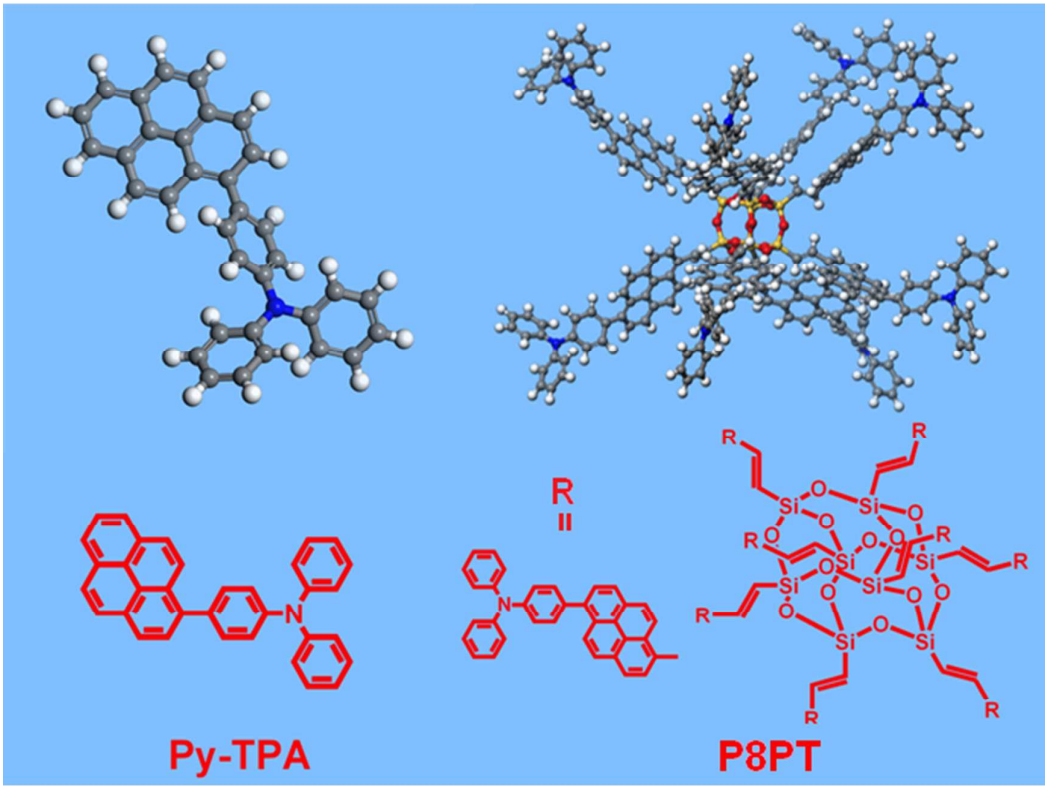

Fig. 1 Chemical structures of **Py-TPA** and **P8PT**.

Table 1 Optical properties and energy level data of **P8PT** and **Py-TPA**.

	Solution		Thin film			
					LUMO (eV)	**HOMO (eV)**
	λ_{Abs}	λ_{Em}	$\lambda_{Abs.}$	λ_{Em}		
P8PT	383	511	417	515	-2.77	-5.70
Py-TPA	359	468	379	475	-2.80	-5.63

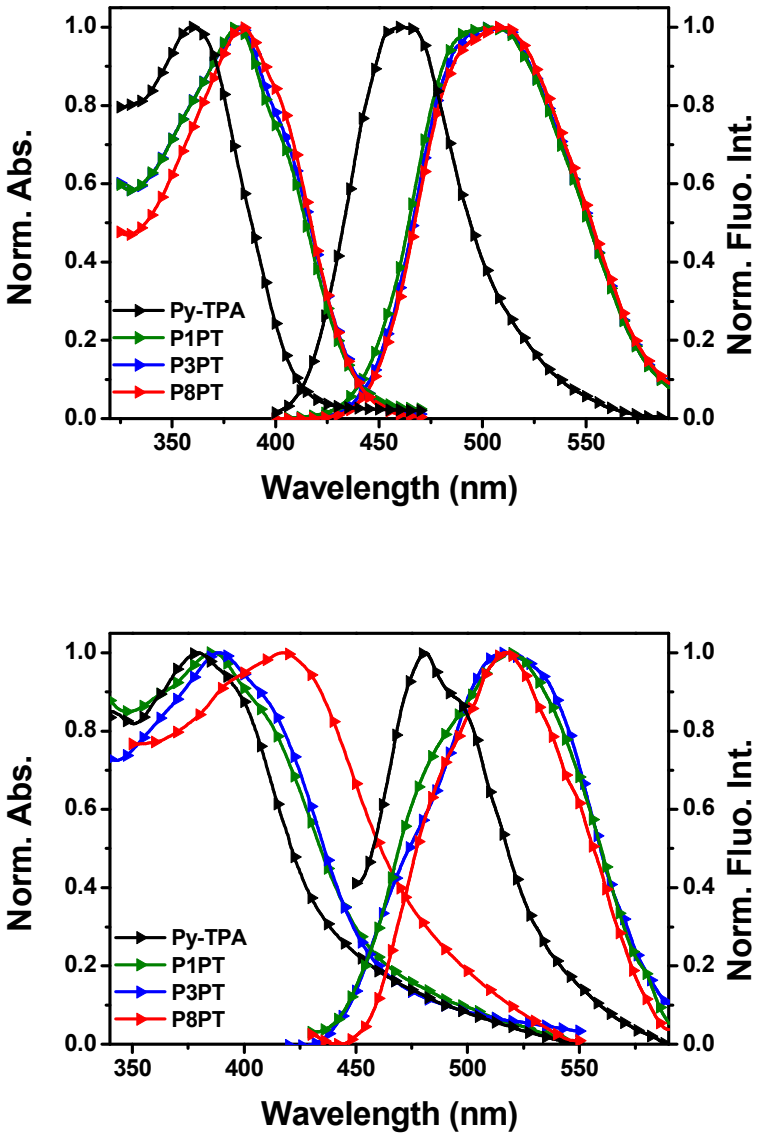

Fig.2 UV-Vis absorption and fluorescence spectra of Py-TPA and POSS-xPyTPA in THF (1×10^{-5} M) (a) and spin-coating films on quartz (b).

Table 2 Optical properties and quenching efficiencies toward NG of **POSS-xPyTPA** and **Py-TPA**.

	Solution		Thin film		Quantum efficiency	Extinction coefficient	Quenching efficiency at 300 s
	λ_{Abs}	λ_{Em}	λ_{Abs}	λ_{Em}			
P8PT	383	511	417	515	0.73	5.26	92%
P1PT	382	510	386	515	0.751	4.36	66%
P3PT	383	510	390	514	0.674	4.48	73%
Py-TPA	359	468	379	475	0.95	4.54	6%

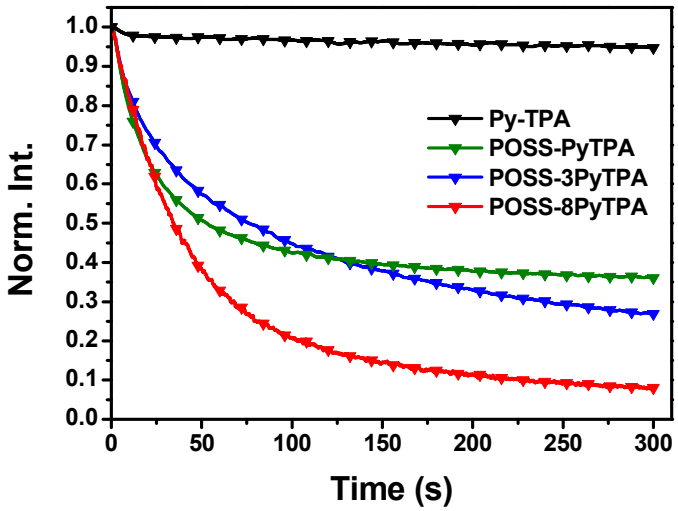

Fig.3 Sensing properties of **Py-TPA, P1PT, P3PT** and **P8PT** film toward saturated NG vapor

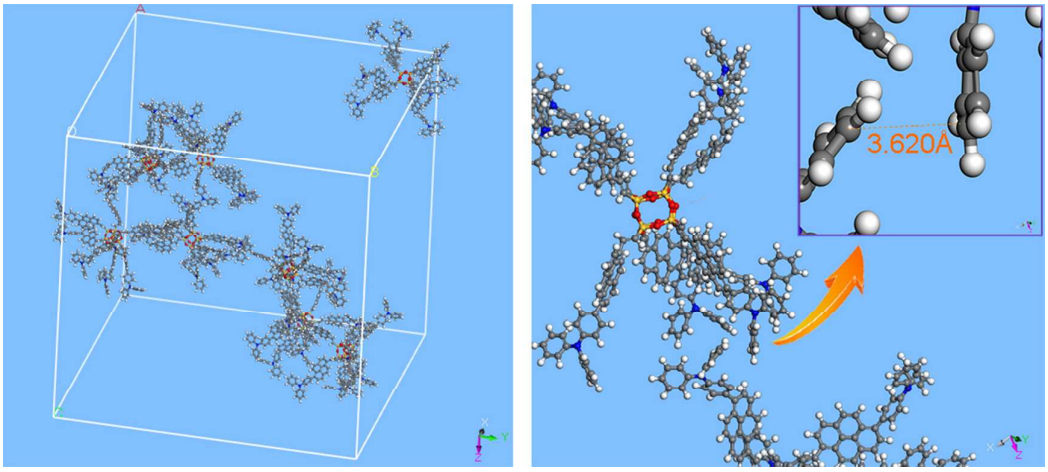

Fig.4 Calculation results of eight **P8PT** molecules in a lattice after 10,000 steps. (use Forcite in Material Studio)

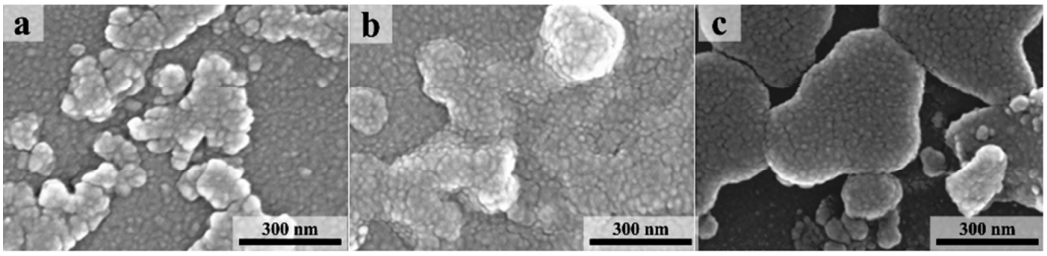

Fig.5 SEM images of **P1PT** (a), **P3PT** (b) and **P8PT** (c) films. All the films were spin coated from their THF solutions with a concentration of 4×10^{-5} mol/L.

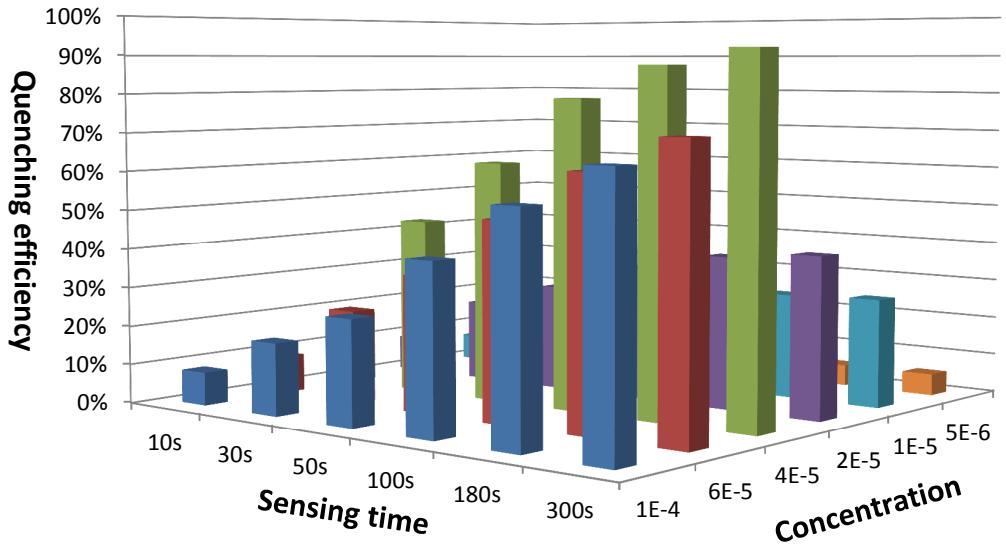

Fig.6 Quenching efficiency of **P8PT** films spin coated from its THF solution with different concentrations for spin-coating.

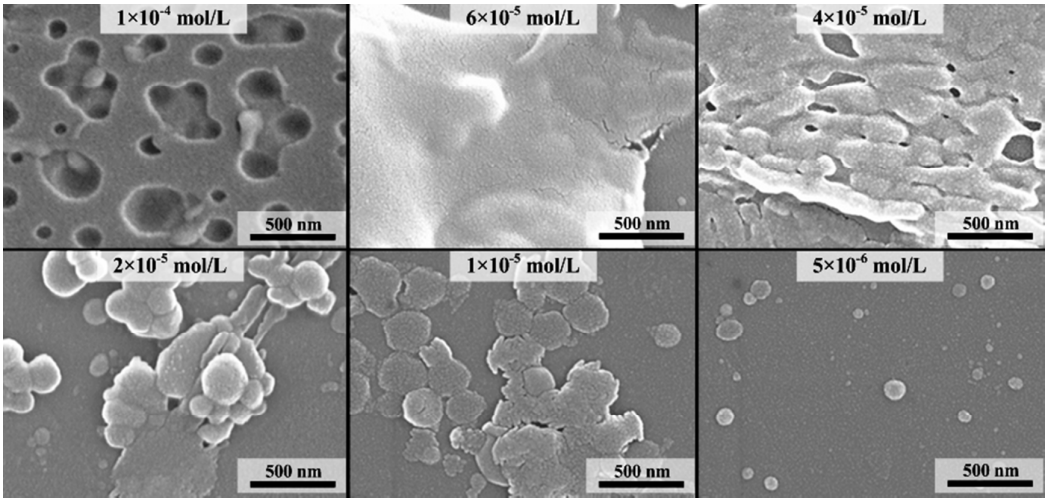

Fig.7 SEM images of **P8PT** films spin coated from its THF solutions of different concentrations (marked on the images).

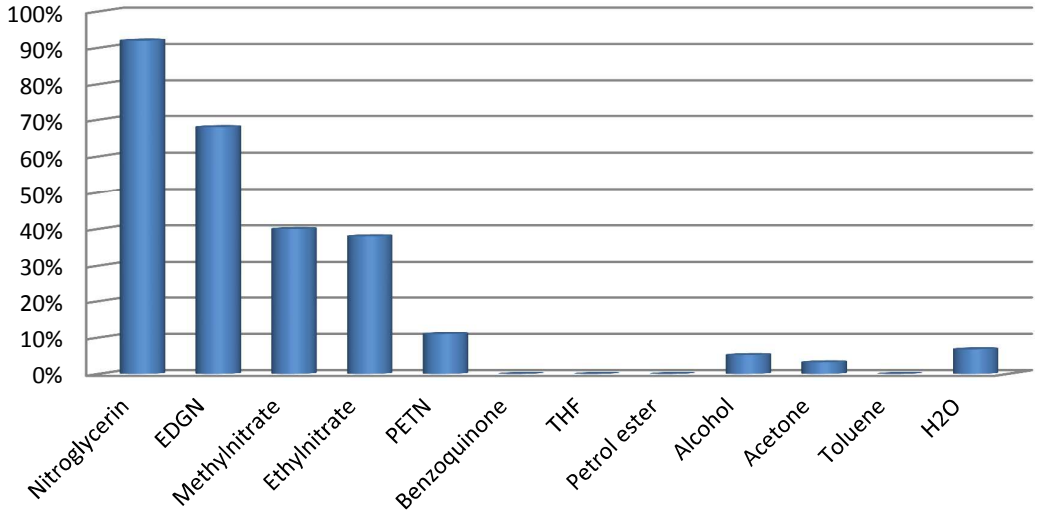

Fig.8 Selectivity of **P8PT** toward a series of nitrate esters and common interferents.

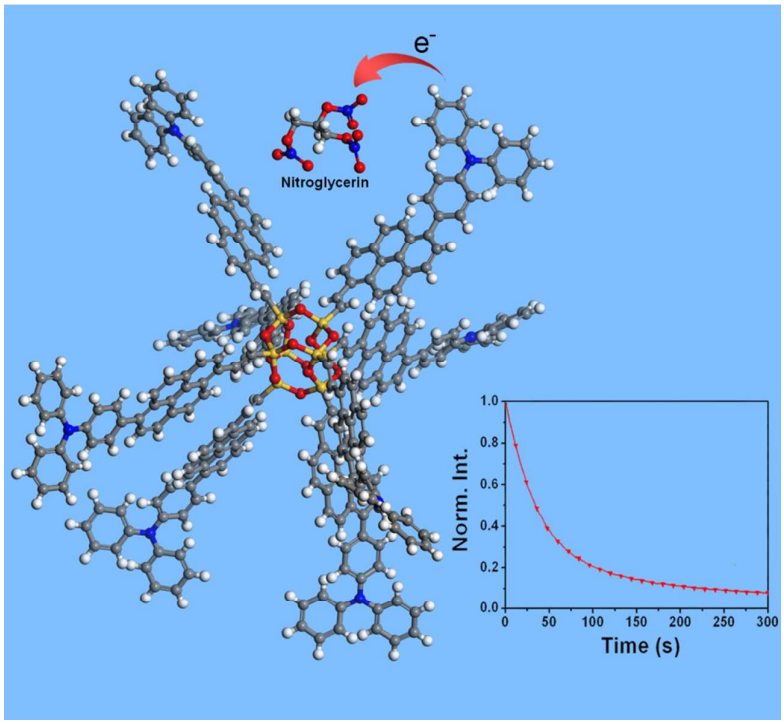

With nano and polar POSS core and eight luminescent branches, P8PT presents excellent fluorescence quenching efficiency to nitroglycerin vapor.